IAC-08-D5.3.6

PREDICTING CHANDRA CCD DEGRADATION WITH THE CHANDRA RADIATION MODEL

Joseph I. Minow
NASA, Marshall Space Flight Center
Huntsville, AL 35812 USA
joseph.i.minow@nasa.gov

William C. Blackwell[1], Joseph M. DePasquale[2], Catherine E. Grant[3], S.L. O'Dell[4], Paul P. Plucinsky[2], Daniel A. Schwartz[2], Bradley D. Spitzbart[2], and Scott J. Wolk[2]

[1]Jacobs Technology, Inc., ESTG, Huntsville, AL 35812 USA
[2]Harvard-Smithsonian Center for Astrophysics, Cambridge, MA 02318 USA
[3]MIT Center for Space Research, Cambridge, MA 02319 USA
[4]NASA, Marshall Space Flight Center, Huntsville, AL 35812 USA

Abstract

Not long after launch of the *Chandra X-Ray Observatory*, it was discovered that the Advanced CCD Imaging Spectrometer (ACIS) detector was rapidly degrading due to radiation. Analysis by *Chandra* personnel showed that this degradation was due to unexpectedly low energy protons (100 – 200 keV) that scattered down the optical path onto the focal plane. In response to this unexpected problem, the *Chandra* Team developed a radiation-protection program that has been used to manage the radiation damage to the CCDs. This program consists of multiple approaches – scheduled radiation safing during passage through radiation belts, the real-time monitoring of space weather conditions, on-board monitoring of radiation environment levels, and the creation of a radiation environment model. This radiation mitigation program has been very successful. The initial precipitous increase in the CCDs' charge transfer inefficiency (CTI) has been slowed dramatically, with the front-illuminated CCDs having an increase in CTI of only 2.3% per year, allowing the ASIS detector's expected lifetime to exceed requirements.

This paper concentrates on one aspect of the Chandra radiation mitigation program, the creation of the Chandra Radiation Model (CRM). Because of *Chandra*'s highly elliptical orbit, the spacecraft spends most of its time outside of the trapped radiation belts that present the severest risks to the ACIS detector. However, there is still a proton flux environment that must be accounted for in all parts of *Chandra's* orbit. At the time of *Chandra's* launch there was no engineering model of the radiation environment that could be used in the outer regions of the spacecraft's orbit, so CRM models the flux environment of 100 – 200 keV protons in the outer magnetosphere, magnetosheath, and solar wind regions of geospace. This presentation describes CRM, its role in *Chandra* operations, and its role in predicting radiation degradation of the ACIS detector.

1.0 Introduction

The *Chandra X-ray Observatory* was launched July 23, 1999 aboard the space shuttle Columbia, joining the Hubble Space Telescope, the Compton Gamma-Ray Observatory, and the Spitzer Space Telescope as one of NASA's "Great Observatories". The initial orbit of 140,000 km apogee and 10,000 km perigee ensured that only a small fraction of the sky is occulted by the Earth for most of the orbital period, and also that the majority of time is spent outside the trapped radiation belts, where the detector backgrounds are high. *Chandra* has been a successful mission, providing sub-arcsecond imaging, spectrometric imaging, and high-resolution dispersive spectroscopy over the x-ray band of 0.08 – 10 keV [*Weisskopf et al.*, 2000].

However, *Chandra's* Advanced CCD Imaging Spectrometer (ACIS) experienced rapid degradation, characterized by increased Charge Transfer Inefficiency (CTI) for the 8 front-illuminated (FI) CCDs, as soon as science operations began. Since the CTI of the back-illuminated (BI) CCDs did not increase, it was immediately recognized that the FI CCDs had suffered damage due to weakly penetrating radiation. *Chandra* personnel determined that this initial damage was created by relatively low-energy (0.1 – 0.5 MeV) protons during 8 passages of the spacecraft through the radiation belts with ACIS situated at the focal plane [*Kolodziejczak et al*., 2000; *O'Dell et al*., 2000]. Although there is no direct line of sight from the free space environment to the *Chandra* focal plane, the low energy protons scatter off the curved x-ray mirrors and onto the focal plane where they lose all their energy and are stopped in the front surface of the detector materials. Only the front illuminated ACIS detectors have exhibited the sensitivity to the low-energy protons, the back illuminated CCDs in the detector array are performing as planned.

2.0 Radiation Protection Procedure

The *Chandra* team quickly altered operating procedures to respond to the rapid increase in CTI seen in the ACIS FI detectors. The immediate change in operation was to translate ACIS from the focal position during radiation-belt transits and during space weather events, limiting exposure to the low energy protons that scatter down the optical path. There are three mitigation techniques (described below) which have been implemented, successfully limiting additional radiation damage to levels that support a mission of at least 15 years [*Cameron et al*., 2001; *O'Dell et al*., 2007].

2.1 Scheduled Protection

Chandra's science operations and other operations are executed by the on-board computer, using a nominal one-week command load. The command load ensures that ACIS is out of the focal position and is protected during radiation belt crossings. The AP8 trapped proton and AE8 trapped electron radiation belt models are used to determine the radiation belt boundaries, with an additional 10-ks pad added to account for variations in the radiation belts not included in the models, especially the outer electron belt boundary. The Chandra Radiation Model (CRM) described in this paper is used in conjunction with historical data from the Electron, Proton, Helium Instrument (EPHIN) instrument on-board the *Chandra* spacecraft since 8 March 2004 to make reductions in the 10-ks pad times, freeing up additional time for science observations [*O'Dell et al*., 2007]. CRM is currently undergoing testing as part of the Offline System (OFLS) software used to generate command loads.

2.2 Autonomous Protection

Because of its highly elliptical orbit, *Chandra* spends the majority of its time outside of the radiation belts with

Table 1. EPHIN Energy Bands

Channel Name	Species	Energy Band (MeV)
E150	e^-	0.25 – 0.70
E300	e^-	0.67 – 3.00
E1300	e^-	2.64 – 6.18
E3000	e^-	4.80 – 10.4
P4	H^+	4.30 – 7.80
P8	H^+	7.80 – 25.0
P25	H^+	25.0 – 40.9
P41	H^+	40.9 – 53.0

their high proton flux. However, in the outer regions of geospace, the spacecraft is still vulnerable to radiation from solar energetic proton events. It is for this reason that the *Chandra* team's radiation management strategy includes an autonomous system that uses EPHIN as an on-board radiation monitor. Table 1 provides the energy response of the EPHIN electron and proton channels [*Blackwell et al*., 2003]. When the count rate in any one of the three EPHIN channels monitored (P4, P41, E1300) exceeds its threshold for a specified number (currently set to 10) of 65.6-s samples, the on-board computer activates a radiation-protection command sequence [*O'Dell et al*., 2007]. EPHIN does not provide direct information on the low-energy (100 to 200 keV) protons that produced the damage to the FI ACIS detectors during the early part of *Chandra's* mission, but it has proven to be a valuable asset in protecting ACIS during solar energetic proton events.

2.3 Manual Intervention

In addition to the autonomous radiation protection system, the Flight Operations Team (FOT) monitors space environment data from NASA spacecraft provided in near-real-time by using a number of spacecraft, most of which are available through the National Oceanographic and Atmospheric Administration (NOAA) Space Environment Center (SEC) to assure the CTI increase is within program acceptable limits [*Cameron et al*., 2001, *O'Dell et al*., 2002].

The proton monitor aboard the *Geostationary Operations Environmental Satellites* (*GOES*) and the *Advanced Composition Explorer* (*ACE*) spacecraft's Solar Isotope Spectrometer (SIS) operating at L1 provide measurements of proton flux at energies of several MeV. The *GOES* and *ACE* data thus provide information to *Chandra* personnel on proton environments similar to those measured by EPHIN between communications with *Chandra*. Proton flux measurements as low as 1 MeV are available in near-real-time from ESA's XMM-*Newton* spacecraft, which is in an orbit similar to

Chandra's. The *ACE* Electron, Proton, and Alpha Monitor (EPAM) provides the solar wind's low energy proton spectrum (0.05 – 2 MeV). EPAM's 0.14 MeV proton flux is used by CRM to estimate *Chandra's* proton environment throughout its orbit, in the solar wind, magnetosheath, and magnetosphere.

3.0 The Chandra Radiation Model

Even when *Chandra* is outside of the radiation belts, spacecraft can be exposed to a significant proton environment. There are episodic injections of plasma from the magnetotail during substorms and major magnetic storms that can increase proton flux in the energy band of concern (100 – 200 keV) by orders of magnitude in the outer magnetosphere. Also, there are 100-200 keV protons found outside of the magnetosphere in the dusk and dayside magnetosheath, or even upstream of the bow shock, since "leakage" across the magnetopause is one of the loss mechanisms for magnetospheric plasma. Another source of potentially dangerous particles are the energetic protons from solar particle events. Because of their energies, solar energetic protons are a concern not only while *Chandra* is in the solar wind, but they also pose a risk while the spacecraft is in the magnetosheath or in the outer magnetosphere. Energetic solar protons easily traverse the bow shock and magnetosheath with little variation in flux and can even penetrate the low magnetic field regions of the outer magnetosphere.

Unfortunately, there is no direct measurement of the low-energy protons available on-board *Chandra*. EPHIN's lowest proton energy channel samples energies of 4.3-7.8 MeV, well above the 100-200 keV proton energies that pose a risk for the ACIS instrument. Even though there is no on-board monitoring of 100-200 keV proton flux along the spacecraft's orbit, the EPHIN channels that are used as radiation monitors have proven to be very useful to monitor for solar energetic proton events and enhanced magnetospheric flux environments during geomagnetic storms. Because of *Chandra's* highly elliptical orbit, it spends a considerable amount of time out of the solar wind and in the Earth's outer magnetosphere and magnetosheath, and there is a need for an engineering-level proton flux environment model for these regions.

The Chandra Radiation Model (CRM) was developed in response to this need for an ability to predict the 100-200 keV proton flux along its orbit [*Blackwell et al.*, 2000, 2003]. The NASA standard trapped proton AP-8 [*Sawyer and Vette*, 1976] and electron AE-8 [*Teague and Vette*, 1974; *Vette*, 1991] models are used by the *Chandra* program to determine the mean locations of the very energetic radiation belts but are not designed to calculate the low energy protons in the outer magnetosphere. CRM is the first engineering-level ion environment model for the outer magnetosphere, and it is designed for use both as a scheduling tool for planning science observations for periods up to three weeks and for a real-time environment model for estimating low energy proton environments.

CRM is a database driven model that uses proton flux measurements from research satellites that sample the magnetosphere, the magnetosheath, and the solar wind. The *Geotail* satellite covers the near Earth region of

Table 2. EPIC/ICS Energy Bands

Channel/ Species	Energy Band (keV/e)	Sector (deg)	Time Resolution Original[a] (sec)	Database[b] (sec)
P2/H^+	58.1 - 77.3	22.5	6	288
P3/H^+	77.3 - 107.4	22.5	48	288
P4/H^+	107.4 - 154.3	22.5	48	288
P5/H^+	154.3 - 227.5	22.5	48	288
P6/H^+	227.5 - 341.6	22.5	48	288
P7/H^+	341.6 - 522.5	22.5	48	288
P8/H^+	522.5 - 813.5	22.5	48	288
P9/H^+	813.5 - 1560.8	22.5	96	288
P10/H^+	560.8 - 3005.4	22.5	96	288

[a]Time resolution of original data.
[b]Time resolution of spin averaged data obtained

Table 3. CEPPAD/IPS Energy Bands

Channel/ Species	Energy Thresholds (keV) Set 1 Min	Set 1 Mid	Set 2 Min	Set 2 Mid
0/H^+	16.8	18.9	13.9	15.6
1/H^+	21.2	24.4	17.5	19.9
2/H^+	27.9	32.4	22.6	26.2
3/H^+	37.5	43.1	30.3	35.4
4/H^+	49.6	57.2	41.4	48.1
5/H^+	65.9	76.0	55.9	55.2
6/H^+	87.7	102.0	75.9	88.4
7/H^+	118.0	138.0	103.0	121.0
8/H^+	161.0	188.0	142.0	168.0
9/H^+	221.0	259.0	198.0	234.0
10/H^+	303.0	355.0	277.0	327.0
11/H^+	417.0	489.0	387.0	459.0
12/H^+	574.0	674.0	543.0	643.0
13/H^+	791.0	929.0	762.0	903.0
14/H^+	1091.0	1281.0	1071.0	1269.0
15/H^+	1505.0	2000.0	1505.0	2000.0

geospace from 10 Re to 30 Re orbit close to the ecliptic plane, sampling all three plasma phenomenology regions. The Comprehensive Energetic Particle and Pitch Angle Detector (CEPPAD) Imaging Proton Spectrometer (IPS) instrument on the *Polar* satellite provides data on the high inclination plasma environments within the magnetosphere. Table 2 the available *Geotail* EPIC/ICS energy channels of which only the P3, P4, and P5 values are used in the CRM model. The *Polar* CEPPAD/IPS energy channels are given in Table 3 from which the P6, P7, and P8 values are used in CRM. Examples of proton flux measurements as a function of Kp are shown in Figure 1 and for comparison, the CRM proton flux values as a function of K_p geomagnetic activity index from the CRM Version 2 (V2) are shown in Figure 2.

Blackwell et al. [2000] describes the original development and implementation of the CRM V1 model using the *Geotail* data. Updates to CRM which added the *Polar*/CEPPAD measurements to the *Geotail* flux measurements is described in *Blackwell et al.* [2003]. Section 3.1 is a brief overview of the technical approach used in development of CRM. Section 3.2 shows examples of model results and section 3.3 describes database upgrades to the magnetosphere and magnetosheath environments in CRM implemented to address an issue of solar particle events included in the databases in the original versions of the model. Section 4.0 shows that the CRM predictions of the degradation rate of the ACIS detectors on-board *Chandra*.

3.1 Technical Approach

CRM is an empirical model that uses databases of satellite measurements of ion flux. Inputs to the model are: location in space, date and time of year, and the K_p geomagnetic index. The software returns values of the ion flux for user selected percentile levels (e.g., the maximum flux value that would be predicted to occur 50% or 90% of the time).

Originally, CRM used a technique of adopting only the physical location of 100 keV to 200 keV ions to fill an empirical model database [*Blackwell et al.*, 2000] to estimate the low energy radiation environment encountered by the *Chandra X-Ray Observatory* satellite [*O'Dell et al.*, 2000]. This early version of CRM used a near-neighbor approach to estimate the flux at the spacecraft location for the three different phenomenological regions: solar wind, magnetosheath, and magnetosphere. Two separate space environment models are used to calculate magnetopause and bow shock boundary locations in CRM. The magnetopause model is from the Tsyganenko geomagnetic field model [*Tsyganenko*, 1995] and the bow shock model used is from a model by Bennett et. al. [*Bennett*, 1997]. The first version of CRM calculated ion flux values as a function of K_p but was limited both in its range of spatial application (-8 Re < Z_{GSM} < +15 Re) and particle energy (100 keV to 200 keV protons.

A major update to the CRM software was made, which implements a streamline/fieldline mapping algorithm that propagates flux from an observation location to other regions of the magnetosphere based on convective ExB and ∇B-curvature particle drift motions in electric and magnetic fields. This allows for the database to be more completely filled and to maximize the limited data available during high K_p periods or in areas of the magnetosphere with little satellite coverage. The modeling approach used in CRM, while applicable to other ion energies, has been focused on the limited range of ion energies identified as a problem for *Chandra* [*Kolodziejczak et al*., 2000]. Figure 3 shows the major software modules in CRM.

3.1.1 Model Implementation

Since ion flux environments in the outer magnetosphere are complex and variable, traditional techniques used to create trapped particle models (e.g., simple B-L flux mapping) cannot be used in magnetospheric regions where the geomagnetic field is highly perturbed and is significantly different than the dipole configuration. There is good correlation between K_p and the ion flux in the outer magnetosphere, but the spatial regions sampled by spacecraft is very sparse during periods when the magnetic activity level is high (with correspondingly high ion flux). Since it is not possible to have a model based strictly upon spacecraft measurement of the ion flux levels, that provides good coverage of all spatial regions of interest, the approach is a combination of database and analytical techniques that fill in the spatial gaps while at the same time maintaining a direct link to the satellite measurements. CRM uses a combination of analytical and database driven models, driven by the K_p proxy parameter of geomagnetic activity levels that provides for correlation of magnetospheric particle flux with geomagnetic disturbances.

3.2.2 Database Generation

The model's database generation is a computationally intensive process that requires mapping all flux values in the Polar and Geotail data sets. Separate databases are required for each energy, K_p value, or other input parameter, requiring significant computer resources to generate the model. However, the runtime code is computationally efficient since the time consuming calculations take place during database generation. Database generation is implemented in three steps:

Step 1: A database of "streamline" position points is created that trace out the drift path available to charged particles while conserving both the total energy and the first adiabatic invariant (the magnetic moment) as they propagate through the magnetosphere. The Tsyganenko geomagnetic field model [*Tsyganenko*, 1995, 1997; *Tsyganenko and Stern* 1996] is used since it provides magnetic field values as a function of solar wind plasma parameters and geomagnetic disturbance values. Figure 4a shows Tsyganenko total field intensity |B| in the Zgsm = 0 plane.

The McIlwain K_p-dependent model [*McIlwain*, 1986] which includes both the convective and co-rotating contributions to the electric potential is used to calculate the electric field. Magnetic field lines are treated as equipotential lines, which allows the potential at the equatorial plane to be mapped to higher magnetic latitudes. Figure 4b shows an example output from the McIlwain geoelectric potential model.

Streamlines are found by minimizing deviations in energy and magnetic moment along the test particle's drift trajectory. These actions are based upon the calculated environments for the magnetic and electric fields for a range of activity levels, conserving particle magnetic moment and energy at each step in the calculation. Figure 5a shows an example of streamlines created for the electric and magnetic fields given in Figure 4. The database generation process uses a much higher number of streamlines than shown in the figure. The streamlines compare favorably to the flux distributions in the data sets as shown in Figure 5b where EPIC/IPS proton flux in the 100-200 keV energy range (for $2 \leq K_p \leq 4$) is projected onto the equatorial plane.

Conserving magnetic moment only applies when the guiding center approximation is valid, that is, where the Larmour radius is smaller than scale size variations of the magnetic field. Figure 6 shows a comparison of the streamlines with satellite measurements of magnetospheric ion flux, demonstrating that the streamline contours generated analytically are in good agreement with the spacecraft flux measurement data (ignore the streamline artifacts in the data "hole").

Step 2: A database of pointers is created that allows for the rapid mapping of a satellite particle flux measurement to a streamline. This cross-referencing database uses spatial volume elements that are at a much finer resolution than used in the final, runtime database used to perform flux calculations.

Step 3: The runtime database is created, using particle flux measurements from the *Geotail* and *Polar* spacecraft. Use the region crossing database to associate each spacecraft measurement with a phenomenological region (solar wind, magnetosheath, magnetosphere). This cross-referencing database is used to determine which streamline(s) to attach a given satellite measurement of magnetospheric flux to. The data is binned, based upon K_p the magnetic activity index. The flux is allowed to be mapped up and down the streamline for a relatively small distance, performing range-weighted averaging of the particle flux.

3.2 Model Results

The runtime database generation process is a computationally intensive process, but once the database is completed the code itself is computationally efficient and runs very quickly. Figure 7 gives examples of streamline mapped output from CRM. Streamlines shown in Figure 6 are used for the K_p = 3 case in this example while appropriate streamlines are computed for the other K_p values.

3.3 Solar Wind Correlated Database Generation

The K_p index is used to correlate CRM output with the proton flux measured in the magnetosphere during geomagnetic substorms, and is also a useful correlate for the ion flux leakage from the magnetosphere into the magnetosheath. However, the penetration of solar event protons is another source of proton flux that is not well correlated with K_p in these regions.

A correlation study was performed which demonstrated that the proton flux measured by the *Polar* and *Geotail* spacecraft in the magnetosphere is strongly correlated with the 0.14 MeV solar proton flux measured by the *ACE*/EPAM instrument at L1 (Fig. 8). Since early versions of the CRM database made no attempt to treat the environments due to solar protons separately from the magnetosheath and magnetosphere environments, they were included incorrectly in the K_p-correlations, producing additional scatter (noise) in the calculations. Figure 8 shows that flux measurements in the magneotsphere are dominated by the proton flux created by geomagnetic activity for low solar proton flux levels, but the solar event flux dominates the outer magnetosphere ion flux at higher solar proton flux levels.

The results from these correlation studies led to the development of new databases for the magnetosphere and magnetosheath regions. These new databases keep the K_p correlation used in earlier CRM databases, but they only contain *Geotail* and *Polar* flux measurements during periods when the solar proton flux measured by

ACE/EPAM is below a threshold level (100 protons/cm^2-sec-sr-MeV), allowing the user to add the effects of solar proton events to CRM output.

Example output from the updated CRM is shown in Figure 9. The CRM V2.3 software is still used to exercise the new databases, Since the only modifications were to the flux database, no change was required to the CRM runtime software. However, because it is necessary for the solar event proton flux to be added to the CRM model predictions, the options available to the user are limited.

There is no CRM database for the solar wind region when the K_p +ACE correlation case is selected. The user must supply the appropriate solar proton flux value for the solar wind region. If the K_p +ACE correlation case is selected to calculate the proton flux in the magnetosheath region, the user must choose to run the option where the sum of the magnetosheath database driven model is added to the appropriately scaled user supplied solar wind flux value. If the K_p +ACE correlation case is selected to calculate the proton flux in the magnetosphere region, the user must choose to run the option where the sum of the magnetosphere database driven model is added to one half the user supplied solar wind flux value.

The Chandra Science Operations Team and Flight Operations Team use a conservative approach to combine the real-time ACE/EPAM data with the near-real-time SWEPAM- K_p driven CRM output [*O'Dell et al., 2007*]:

1. Solar wind $F_1(t) = F_{EPAM}(t)$
2. Magnetosheath $F_2(t) = 2 \times F_{EPAM}(t) + F_{CRM}(K_p (t))$
3. Magnetosphere $F_3(t) = F_{CRM}(K_p (t)) + ½ \times F_{EPAM}(t)$.

4.0 CRM Prediction of CCD Degradation

Radiation damage in CCDs can result in an increase of charge traps. As charge is transferred to the readout, a portion of the charge can be captured by the traps and gradually re-emitted. This can result in a reduction of the charge transferred from the charge packet. The charge transfer inefficiency (CTI) is the fractional charge loss per pixel and can be used as a measure of radiation damage in the ACIS detectors. The protons that scatter down the telescope's optical path onto the focal plane effects the charge deposited on the CCD, so the measured CTI is a function of the particle fluence [*Grant et al*., 2005].

A program (CRM_HistACIS) was developed to examine the use of *Chandra's* mission proton fluence calculated by CRM to predict the degradation of the ACIS front illuminated detectors. The *Chandra Science Operations Team* (SOT) provided a number of items used to perform this analysis, including: the *Chandra* ephemeris, the CTI values measured on-board the spacecraft, the times that the High Energy Transmission Grating (HETG) and the Low Energy Transmission Grating (LETG) are in the optical path, and the times that ACIS is in the focal plane. Other information used includes data files containing records of the magnetic activity index (K_p) and proton flux values from the Advanced Composition Explorer (ACE) spacecraft in orbit about the Earth – Sun L2 point.

CRM_HistACIS calculates the *Chandra* 100 – 200 keV proton fluence based on the actual spacecraft locations and the historical values of K_p. The proton fluence is not integrated during times when the ACIS detector was in a protected position. Also, the code models the placement and removal of the gratings (LETG or HETG) in the optical path and the corresponding effect on the transmission of protons to the focal plane. A CRM to CTI transfer function is found by performing a least-squares linear fit to the measured CTI and the CRM fluence. The mission fluence and the corresponding CTI are calculated. Figure 10 shows the integrated fluence and Fig. 11 shows the comparison of the CTI calculated with CRM and the CTI based on measurements made on-board the spacecraft, demonstrating that CRM can be used to predict long-term effects of the low energy proton environment on ACIS performance.

5.0 Summary

After a brief period of rapid degradation in the ACIS FI detectors, the *Chandra* team rapidly developed and put into place a set of procedures which have eliminated the problem. A number of tools, including the on-board radiation monitor EPHIN and the NOAA space environment monitoring *ACE* spacecraft in orbit about the Sun-Earth L1 point, are used by *Chandra* personnel to limit ACIS and other instrument exposure to damaging particle radiation. The mitigation procedures in place have successfully limited the CTI degradation of ACIS detectors within levels that will allow the ACIS front illuminated CCDs to provide viable science data at least for a 15 year mission or even longer. To supplement the data provided by multiple space weather sensing spacecraft, the Chandra Radiation Model was created.

CRM is currently in use as a near-real-time proton flux environment analysis tool by the *Chandra* Science

Operations Team and the Flight Operations Team. The CRM code is also undergoing testing as part of the Offline System software for use in scheduling ACIS operations to reduce the radiation belt ingress/egress pad times used as a safety margin for placing ACIS in a protected position. The databases released with earlier versions of CRM used only one correlate, the K_p magnetic activity index. A new database has been created which allows for a better representation of the solar proton flux penetration into the magnetosheath and magnetosphere phenomenological regions of geospace and more fully populates those regions. Calculations of mission fluence with CRM have demonstrated that the code can be used to make accurate predictions of ACIS detector degradation.

Acknowledgements

Geotail EPIC/IPS data was provided by Dr. Richard McEntire and Mr. Stuart Nylund (JHU/APL). Polar CEPPAD/IPS data was provided by Dr. Harlan Spence, Boston University. The *Chandra* ephemeris information was provided by the *Chandra* Science Operations Team (SOT) and Flight Operations Team (FOT). Geomagnetic indices were obtained from the NOAA National Geophysical Data Center. Geotail CPI/Hot Plasma Analyzer data plots were provided courtesy of Dr. Louis Frank and Dr. William R. Patterson, University of Iowa. William C. Blackwell is supported by NASA Contract NNM05AB50C to Jacobs Technology, Inc.

References

Bennett, L., M. G. Kivelson, K.K. Khurana, L. A. Frank, and W. R. Patterson, A model of the Earth's distant bow shock, J.Geophys.Res., 102, 26927, 1997.

Blackwell, W.C., J. I. Minow, S.L. O'Dell, R.M. Suggs, D.A. Swartz, A.F. Tennant, S.N. Virani, & K.M. Warren, "Modeling the Chandra space environment", in *X-Ray and Gamma-Ray Instrumentation for Astronomy XI, Proc. SPIE*, **4140**, pp. 111 – 122, 2000.

Blackwell, W.C., J. I. Minow, S. Smith, W.R. Swift, S.L. O'Dell, and R. Cameron, The Chandra X-ray Observatory Radiation Environment Model, AIAA-2003-1228, 2003.

Cameron, Robert A., David C. Morris, Shanil N. Virani, Scott J. Wolk, William C. Blackwell, Joseph I. Minow and Stephen L. O'Dell, *Shelter from the Storm: Protecting the Chandra X-ray Observatory from Radiation*, ADASS XI, Victoria, BC, Canada, September, 2001.

Grant, C.E., Bautz, M.W., Kissel, S.E., LaMarr, B., and Prigozhin, G.Y., "Long-term trends in radiation damage of Chandra X-ray CCDs" in *UV, X-Ray, and Gamma-Ray Space Instrumentation for Astronomy XIV*, ed. O.H.W. Siegmund, *Proc. SPIE* **5898**, 201-211, 2005.

Kolodziejczak, J.J., R.F. Elsner, R.A. Austin, and S.L. O'Dell, Ion transmission to the focal plane of the Chandra X-ray Observatory, *Proc. SPIE* ,4140, pp. 135 - 143, 2000.

McIlwain, C.E., "A K_p dependent equatorial electric field model," Advances in Space Research, 6, 187 – 197, 1986.

O'Dell, S.L., M.W. Bautz, W.C. Blackwell, Y.M. Butt, R.A. Cameron, R.F. Elsner, M.S. Gussenhoven, J.J. Kolodziejczak, J.I. Minow, D.A. Swartz, A.F. Tennant, S.N. Virani, K. Warren, "Radiation environment of the Chandra X-ray Observatory", in *X-Ray and Gamma-Ray Instrumentation for Astronomy, Proc. SPIE*, **4140**, pp. 99-110, 2000.

O'Dell, S.L., W. C. Blackwell, Jr., R. A. Cameron, J. I. Minow, D. Morris, S. N. Virani, *Managing radiation degradation of CCD's on the Chandra X-ray Observatory*, SPIE 4851-07, X ray and Gamma-ray Telescopes and Instruments for Astronomy (Truemper, Tananbaum), 22-28 August 2002, Hawaii.

O'Dell, S.L., T.L. Aldcroft, W. C. Blackwell, S.L. Bucher, J.H. Chappell, J.M. DePasquale, C.E. Grant, M. Juda, E.R. Martin, J. I. Minow, S.S. Murray, P.P. Plucinsky, D.A. Schwartz, D.P. Shropshire, B.J. Spitzbart, P.R. Viens, S.J. Wolk, *Managing radiation degradation of CCDs on the Chandra X-ray Observatory III*, SPIE **6686**, in *UV, X ray and Gamma-Ray Space Instrumentation for Astronomy XV*, 26-27 August 2007, San Diego.

Parks, G.K., *Physics of Space Plasmas, An Introduction*, Perseus Books, Reading, MA, 1991.

Roederer, J.G., *Dynamics of Geomagnetically Trapped Radiation*, Springer-Verlag, New York, NY, 1970.

Sawyer, D.W., and J.I. Vette, "AP-8 Trapped Proton Environment for Solar Maximum and Solar Minimum," National Space Science Data Center, NASA Goddard Space Flight Center, NSSDC/WDC-A-R&S 76-06, 1976.

Teague, M.J., and J.I. Vette, "A model of the trapped electron population for solar minimum," National Space Science Data Center, NASA Goddard Space Flight Center, NSSDC 03-74, 1974.

Tsyganenko, N.A. Modeling the Earth's magnetospheric magnetic field confined within a realistic magnetopause, J. Geophys.Res., 100, 5599, 1995.

Tsyganenko, N.A., and D.P. Stern, Modeling the global magnetic field of the large-scale Birkeland current systems, J.Geophys.Res., 101, 27187, 1996.

Tsyganenko, N.A., An empirical model of the substorm current wedge, J.Geophys.Res., 102, 19935, 1997.

Vette, J.I., "The AE-8 trapped electron model environment," National Space Science Data Center, NASA Goddard Space Flight Center, NSSDC/WDC-A-R&S 91-24, 1991.

Weisskopf, M.C., H.D. Tanabaum, L.P. Van Speybroeck, S.L. O'Dell, Chandra X-ray Observatory (CXO): Overview, SPIE **4012**, p. 2-16, X-Ray Optics, Instruments, and Missions III, 27-31 March 2000, Munich.

E-mail address of W.C. Blackwell
William.C.Blackwell@nasa.gov

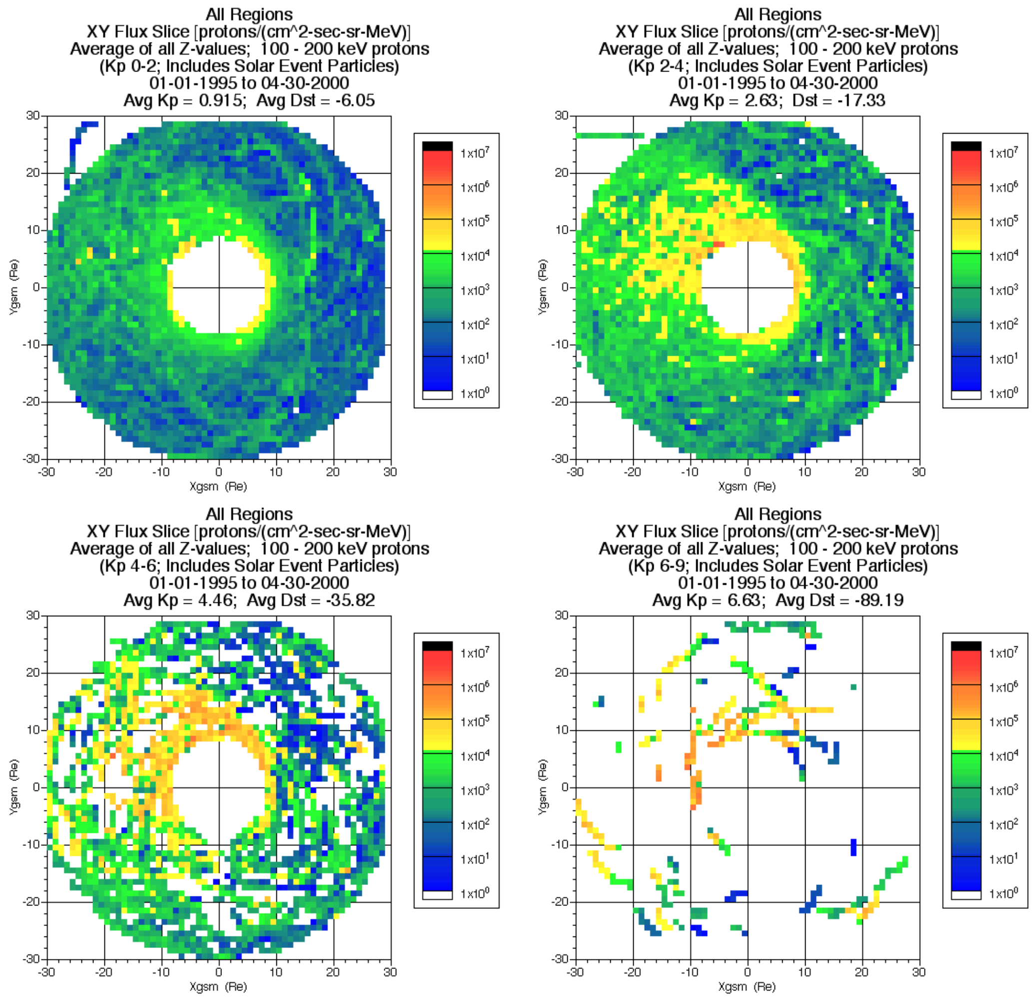

Figure 1. Proton Flux Correlation with Kp. EPIC/ICS ion flux values are projected onto the Z_{GSM} = 0 plane. The "hole" in the center is the perigee altitude of the Geotail spacecraft.

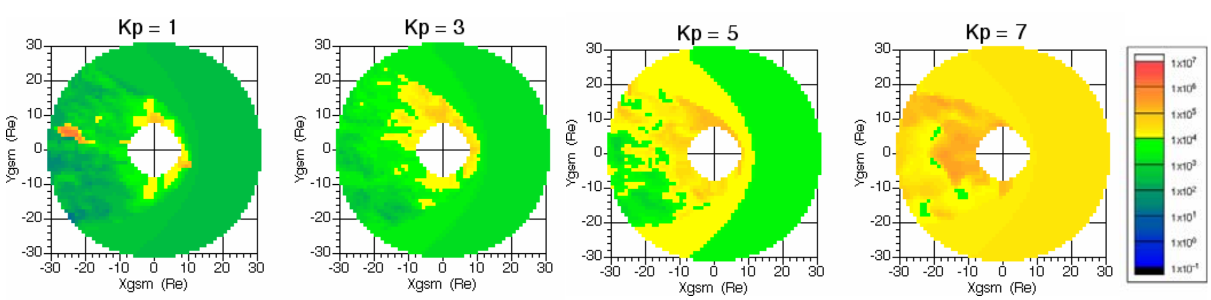

Figure 2. CRM v2 Output. Kp dependent proton flux (in units of #/cm2-s-sr-MeV) is given by the model for protons between 100 keV and 200 keV (adapted from *Blackwell et al.*, 2003).

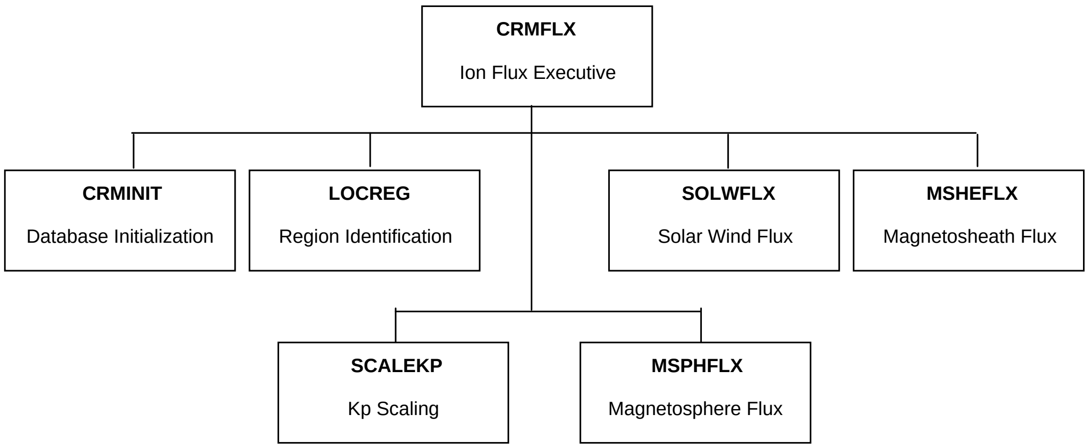

Figure 3. Major software modules in CRM.

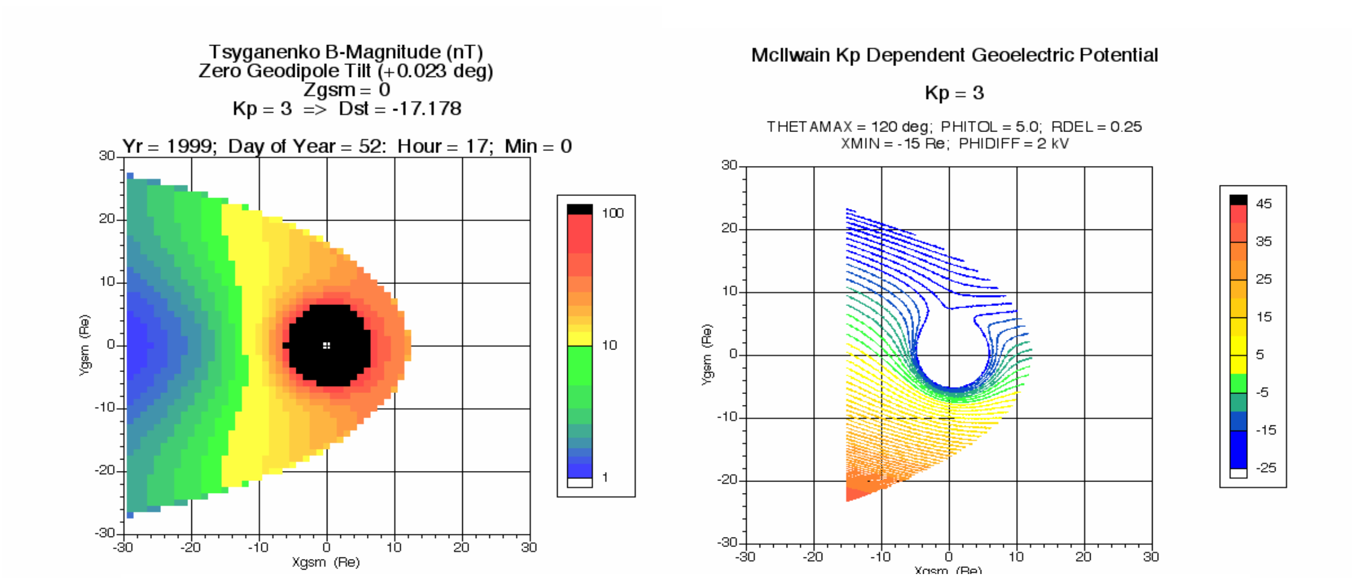

(a) **(b)**

Figure 4. Magnetic and Electric Potential Models. (a) Tsyganenko magnetic field intensity |B| (nT) and (b) geoelectric potential (kV) in the $Z_{GSM} = 0$ plane. These values will be used to compute an example set of streamlines shown in later figures.

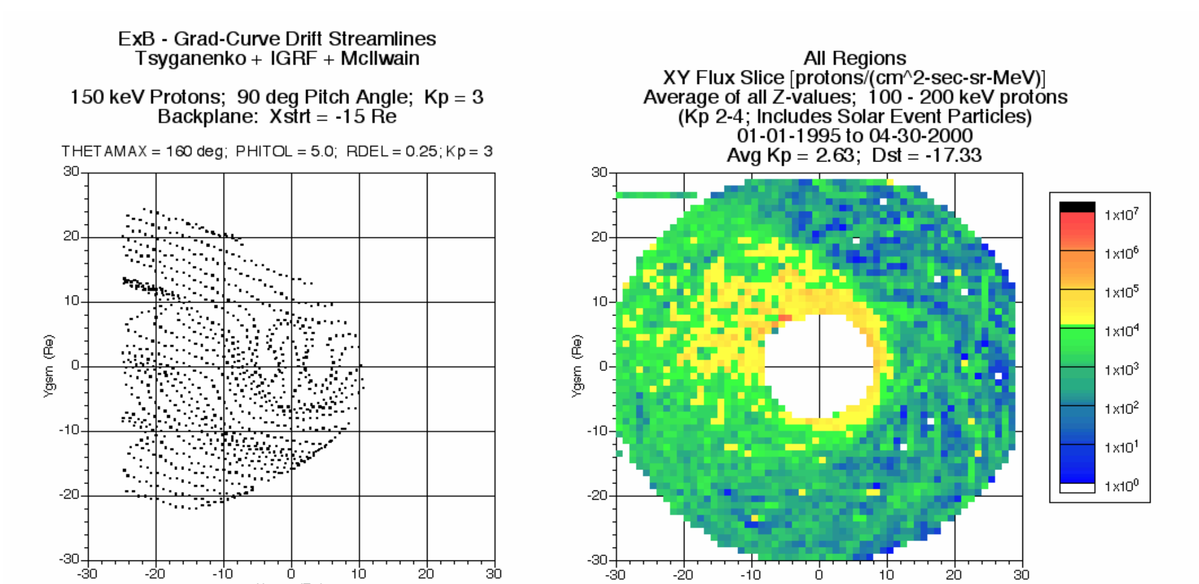

(a) **(b)**

Figure 5. Example Streamlines and Flux Observations. (a) Streamlines generated in Step 2 are projected onto the $Z_{GSM} = 0$ plane and can be compared to (b) *Geotail* spacecraft flux data for all phenomenological regions (solar wind, magnetosheath, and magnetosphere) without streamline mapping.

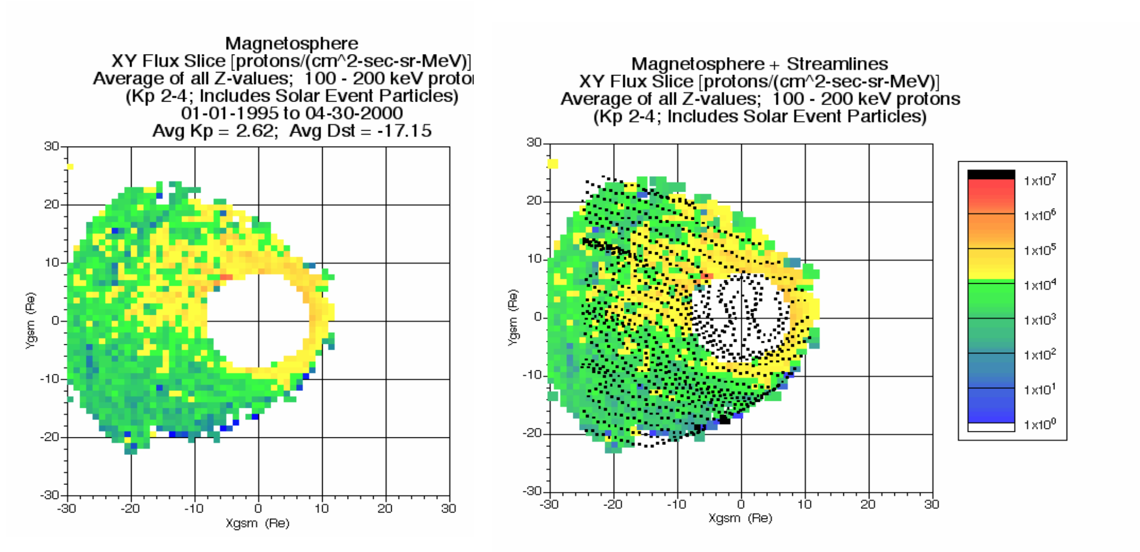

(a) **(b)**

Figure 6. Streamline Overlay on Magnetospheric Ion Flux Distributions. (a) Ion flux within the magnetosphere are projected onto the Zgsm = 0 plane. (b) Streamlines shown in Figure 2a are plotted over the ion flux distribution.

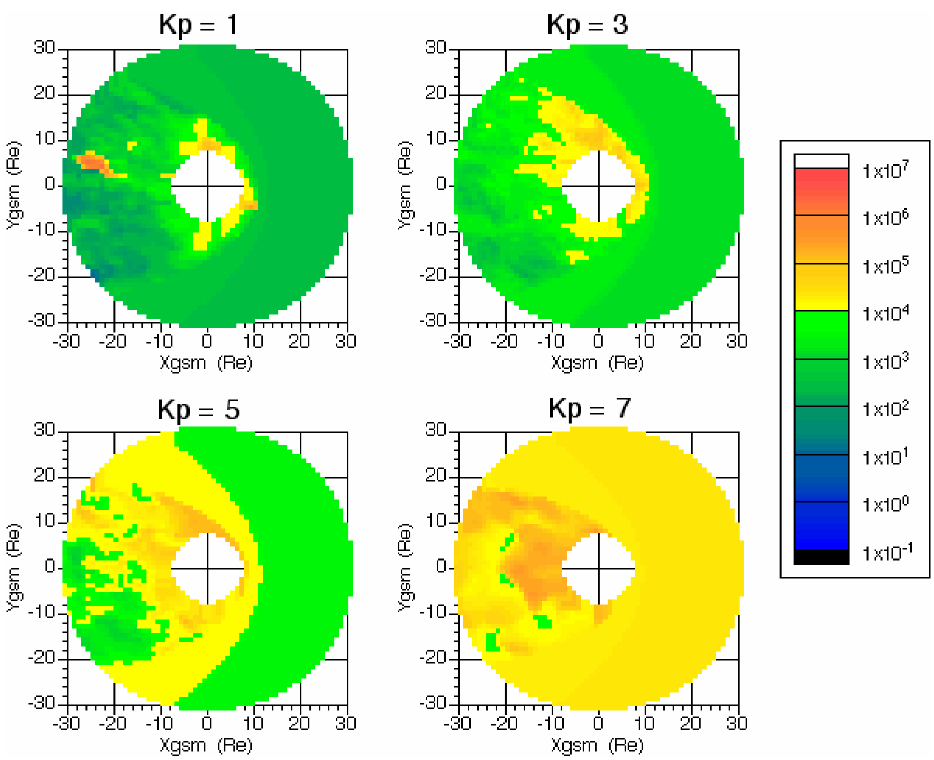

Figure 7. Ion Flux (protons/cm2-sec-sr-MeV) Output from CRM for a Range of K_p Values. Note the inward motion of the model magnetopause for higher Kp values (a property of the Tsyganenko magnetic field model) and the increase in flux.

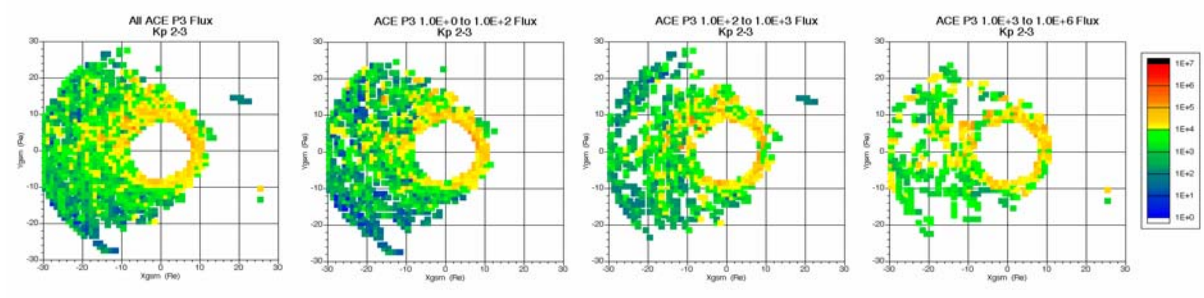

Figure 8. Solar Event Particle Correlation. *ACE* solar proton event correlation with *Geotail* flux data (units of protons/cm2-sec-sr-MeV) inside the magnetosphere for nominal Kp values. At low solar proton flux levels the data is dominated by the proton flux created by geomagnetic activity. At higher solar proton flux levels the solar event flux dominates in the outer magnetosphere.

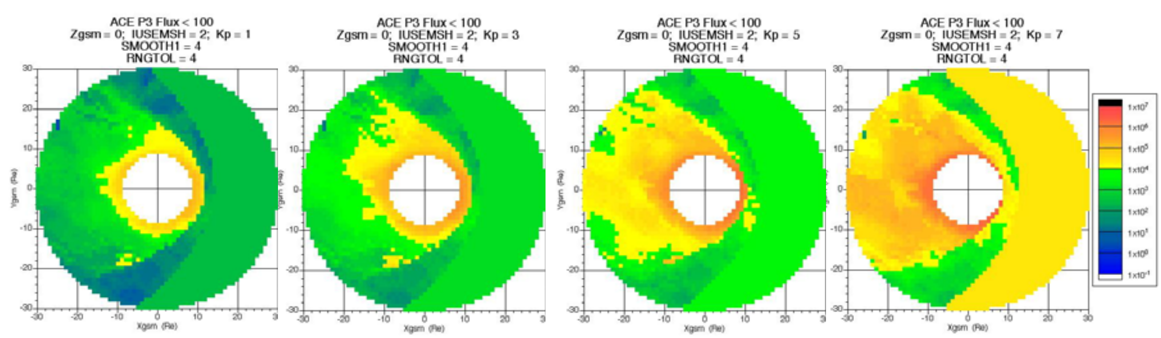

Figure 9. **CRM Output with *ACE* Correlated Database.** Geomagnetic activity variation output from CRM using the new solar event particle correlated databases for the magnetosphere and magnetosheath regions. The original, uncorrelated analytic solar wind model is used for these results.

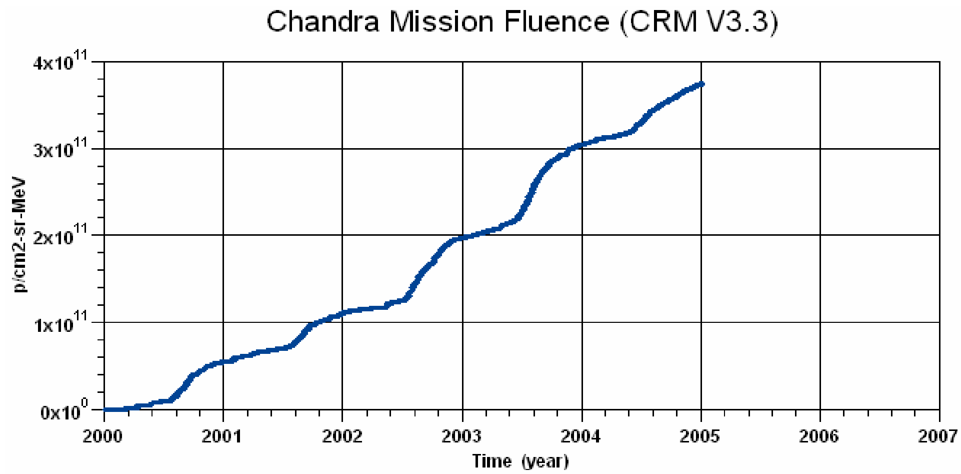

Figure 10. Chandra mission fluence calculated with CRM v3.3, including times when ACIS is in an exposed position and when transmission gratings are in the optical path.

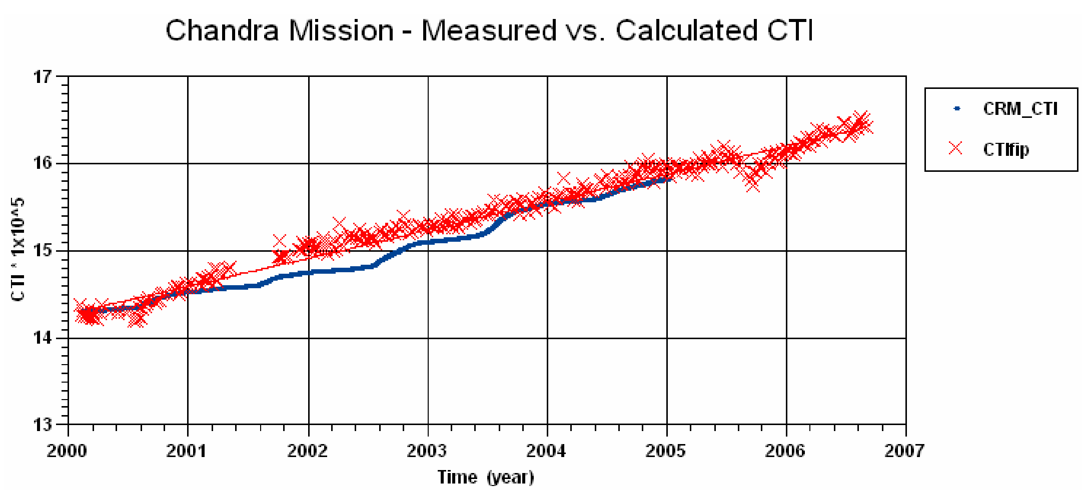

Figure 11. Comparison between the CTI measured on-board Chandra and the CTI based on CRM fluence.

Predicting Chandra CCD Degradation with the Chandra Radiation Model

Joseph I. Minow[1], William C. Blackwell[2], Joseph M. DePasquale[3], Catherine E. Grant4[4], S.L. O'Dell[1], Paul P. Plucinsky[3], Daniel A. Schwartz[3], Bradley D. Spitzbart[3], and Scott J. Wolk[3]

[1]NASA, Marshall Space Flight Center, Huntsville AL USA
[2]Jacobs Technology, Inc., ESTG, Huntsville AL USA
[3]Harvard-Smithsonian Center for Astrophysics, Cambridge, MA USA
[4]MIT Center for Space Research, Cambridge, MA USA

59th International Astronautical Congress
Glasgow, Scotland 29 Sep- 3 Oct 2008

Introduction

Today's presentation will:

- Describe the development of the Chandra Radiation Model (CRM)
- Demonstrate CRM application in minimizing radiation damage to Chandra instrumentation

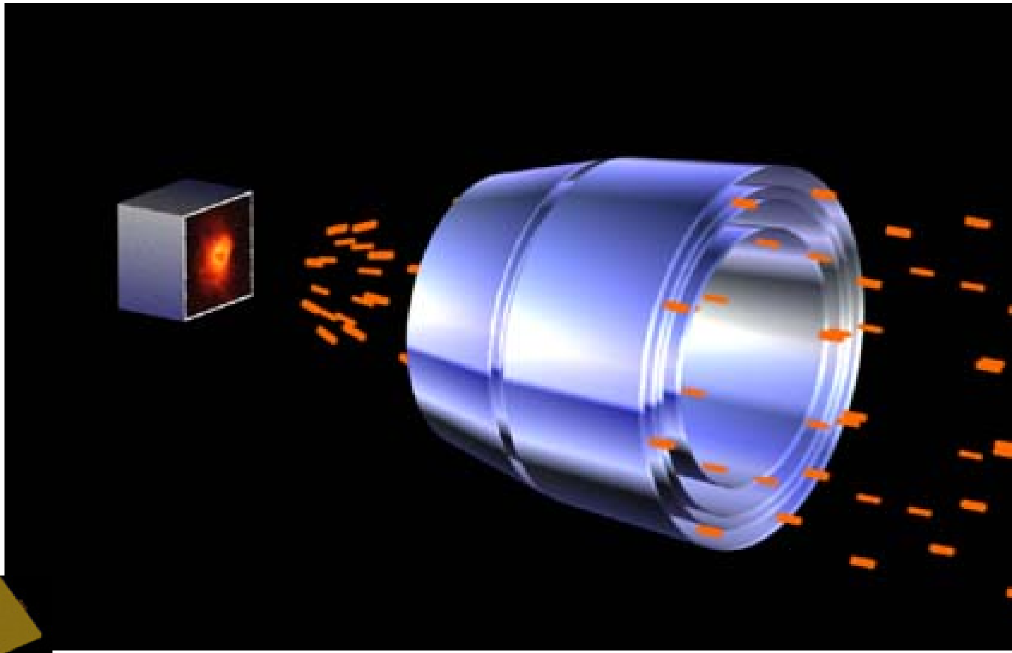

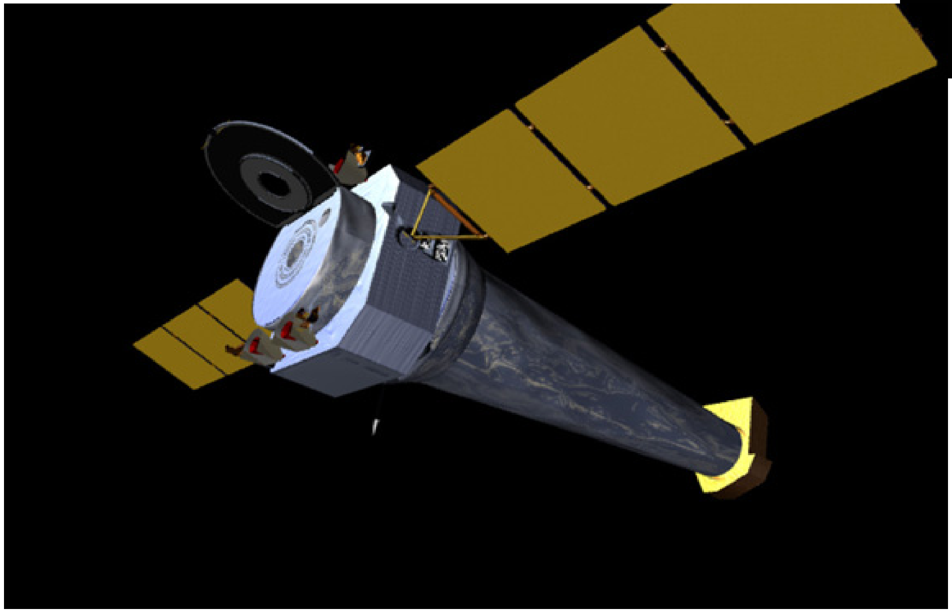

Outline

- Chandra radiation issues
- CRM development
- Fluence estimates

Chandra Orbit in Geospace

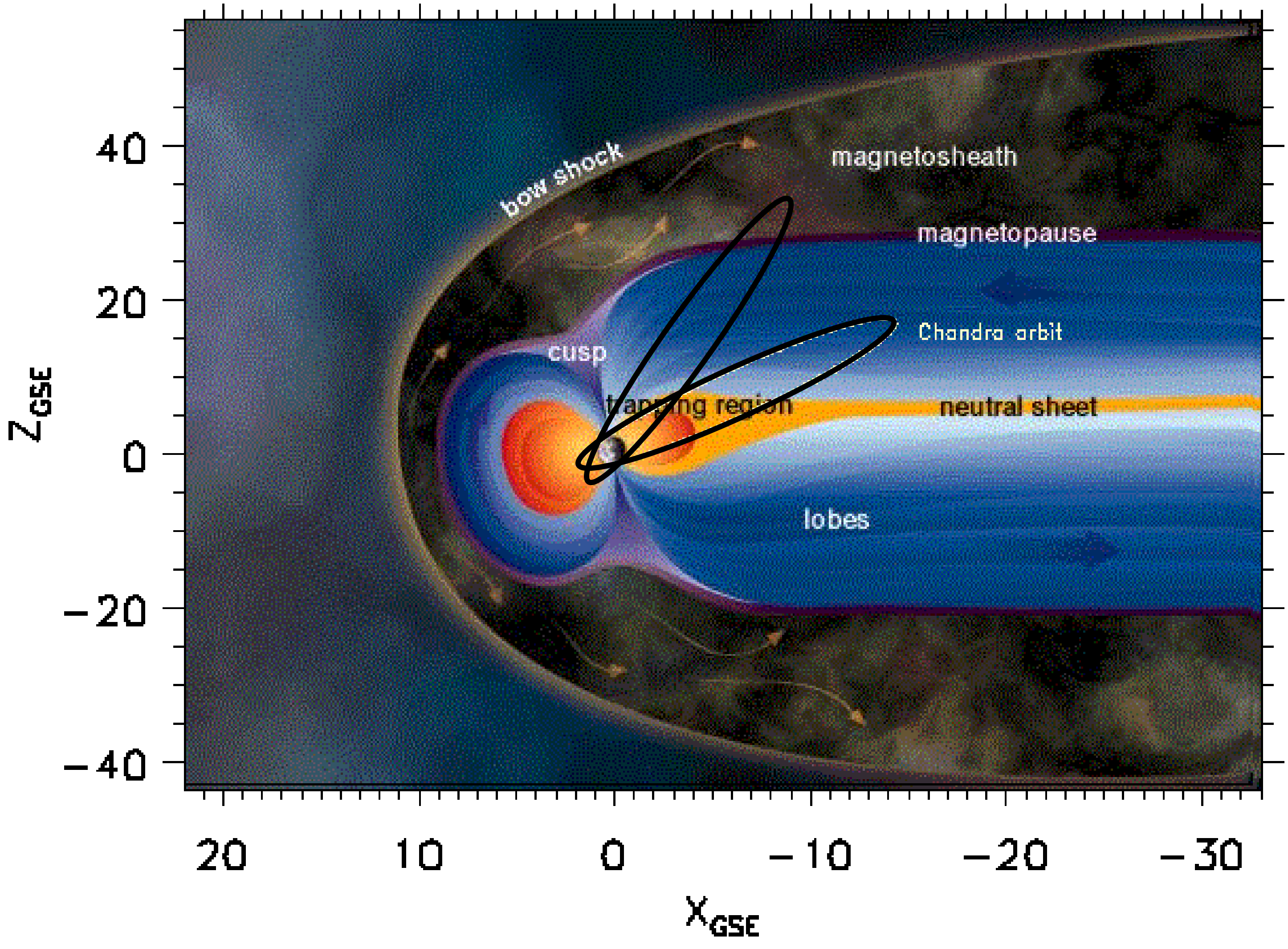

ACIS Radiation Issue

- **Chandra's Advanced Charge Coupled Device Imaging Spectrometer (ACIS) is susceptible to radiation degradation when exposed to energetic protons**
  - **Ion interactions with CCD material generates electron trapping sites in active region of CCD, increases the Charge Transfer Inefficiency (CTI)**
  - **Increased CTI results in reduction of CCD resolution**

- **Energetic proton sources**
  - **Cosmic ray background**
    - **Directly penetrate spacecraft hull, low flux**
    - **Manageable background degradation**

  - **100 to 200 keV protons**
    - **High proton flux trapped in Earth's magnetic field (radiation belt, ring currents)**
    - **keV protons easily shielded, but scatter down the optical path onto CCD detector**
    - **Degradation only occurs on front illuminated CCD's**

- Mitigation
  - **Schedule observations in low proton flux environments**
  - **Move ACIS to shielded position during radiation belt passages**

Environment Model

- **Proton flux model is required to determine safe locations along spacecraft orbit where ACIS detector can be used**
  - **Model must provide proton flux in outer magnetosphere, magnetosheath, and solar wind**
    - AP-8 is appropriate only for trapped protons in radiation belts
  - **Chandra approach was to create a database driven model**
    - CRM is an empirical model of the free field outer magnetosphere, magnetosheath, and solar wind ion fluxes in energy range of interest to CXO

- **Applications for CRM**
  - **Mission planning**
    - Incorporate into the CXO off-line mission planning system to aid in determination of safing times for ACIS detector
    - Provide additional orbit “events” to those determined for radiation belt passage using AP-8 model
  - **Near-real-time environment tool**
    - Assess the ion fluence for individual orbits
    - Tool for management of the CTI ACIS degradation

Data Sources

Geotail

Energetic Particle and Ion Composition (EPIC) Ion composition Spectrometer (ICS) instrument

Polar

Comprehensive Energetic Particle and Pitch Angle Detector (CEPPAD) Imaging Proton Spectrometer (IPS) instrument

Table 2. EPIC/ICS Energy Bands

Channel/ Species	Energy Band (keV/e)	Sector (deg)	Time Resolution Original[a] (sec)	Time Resolution Database[b] (sec)
P2/H^+	58.1 - 77.3	22.5	6	288
P3/H^+	**77.3 - 107.4**	**22.5**	**48**	**288**
P4/H^+	**107.4 - 154.3**	**22.5**	**48**	**288**
P5/H^+	**154.3 - 227.5**	**22.5**	**48**	**288**
P6/H^+	227.5 - 341.6	22.5	48	288
P7/H^+	341.6 - 522.5	22.5	48	288
P8/H^+	522.5 - 813.5	22.5	48	288
P9/H^+	813.5 - 1560.8	22.5	96	288
P10/H^+	560.8 - 3005.4	22.5	96	288

[a]Time resolution of original data.

[b]Time resolution of spin averaged data obtained from Principle Investigator.

Table 3. CEPPAD/IPS Energy Bands

Channel/ Species	Energy Thresholds (keV) Set 1 Min	Set 1 Mid	Set 2 Min	Set 2 Mid
0/H+	16.8	18.9	13.9	15.6
1/H+	21.2	24.4	17.5	19.9
2/H+	27.9	32.4	22.6	26.2
3/H+	37.5	43.1	30.3	35.4
4/H+	49.6	57.2	41.4	48.1
5/H+	65.9	76.0	55.9	55.2
6/H+	**87.7**	**102.0**	**75.9**	**88.4**
7/H+	**118.0**	**138.0**	**103.0**	**121.0**
8/H+	**161.0**	**188.0**	**142.0**	**168.0**
9/H+	**221.0**	**259.0**	**198.0**	**234.0**
10/H+	303.0	355.0	277.0	327.0
11/H+	417.0	489.0	387.0	459.0
12/H+	574.0	674.0	543.0	643.0
13/H+	791.0	929.0	762.0	903.0
14/H+	1091.0	1281.0	1071.0	1269.0
15/H+	1505.0	2000.0	1505.0	2000.0

- Data sets are sparse at high geomagnetic activity
  - Kp < 4 well represented
  - Kp > 4 is sparse
- Example here is
  - Geotail Energetic Particles and Ion Compsition (EPIC) Ion Composition Spectrometer (ICS) records mapped onto equatorial plane
  - 1 Jan 1995 – 30 Apr 2000
- Sparse data utilized through mapping scheme

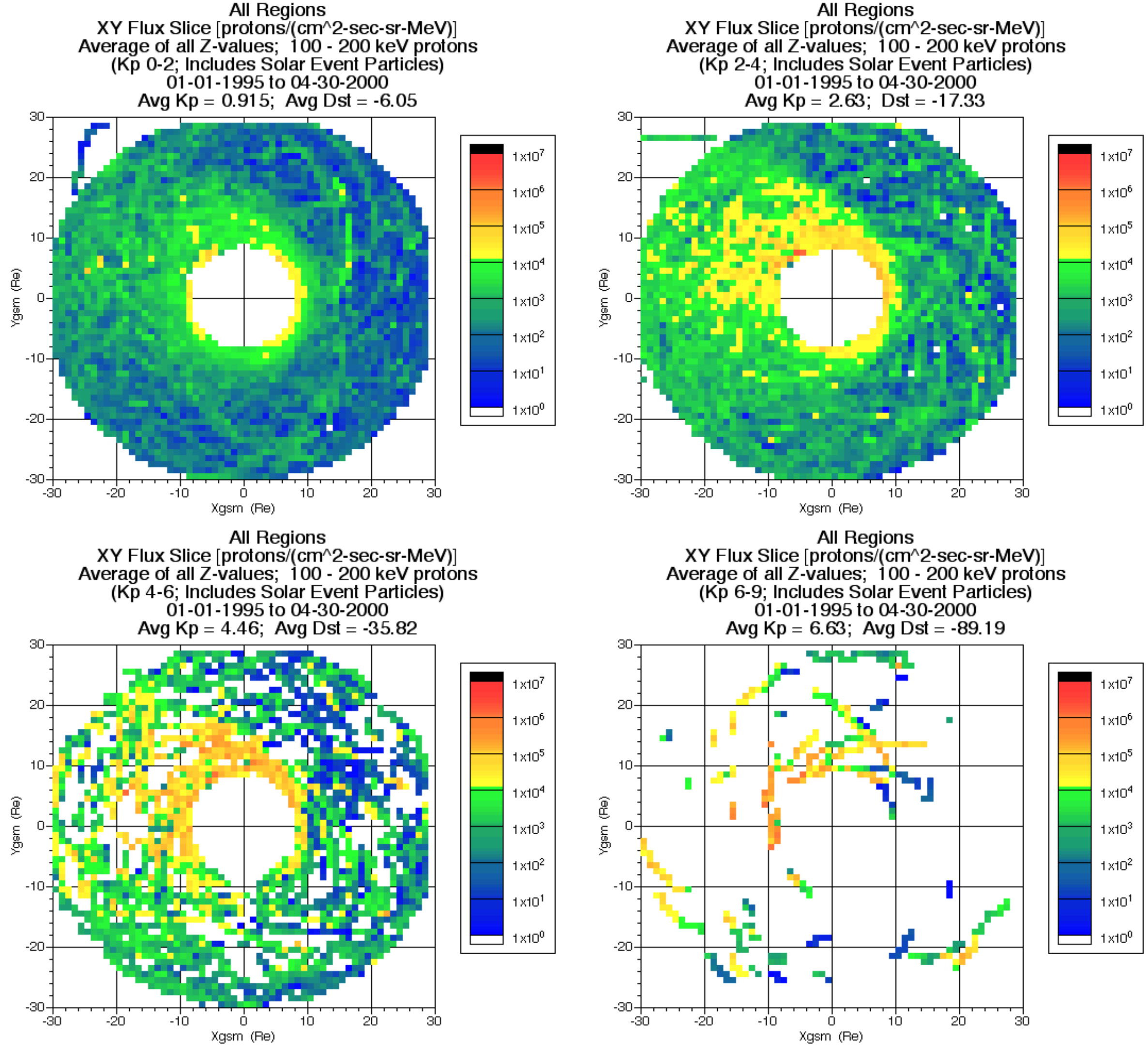

Figure 1. Proton Flux Correlation with Kp. EPIC/ICS ion flux values are projected onto the $Z_{GSM} = 0$ plane. The “hole” in the center is the perigee altitude of the Geotail spacecraft.

Field Line Mapping

1999/200.3 Kp = 3.5 Dst = -20 nT

Solar wind proton flux=1x10^4 #/cm2-sec-sr-MeV Region =magnetosphere

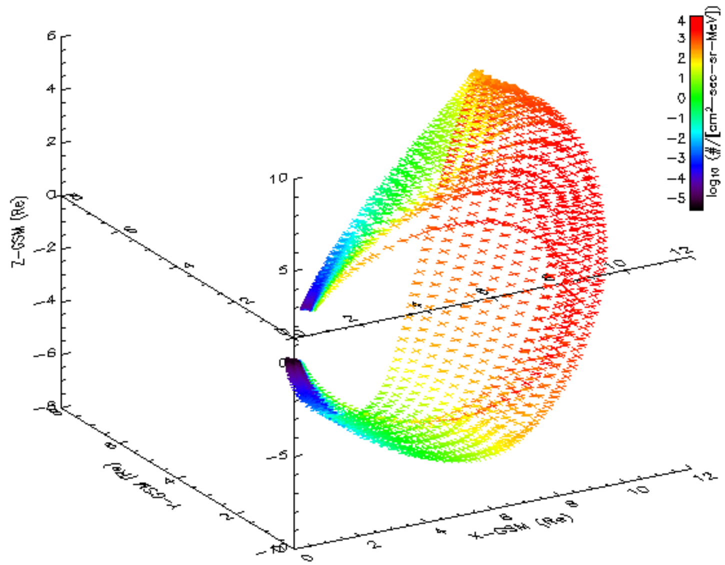

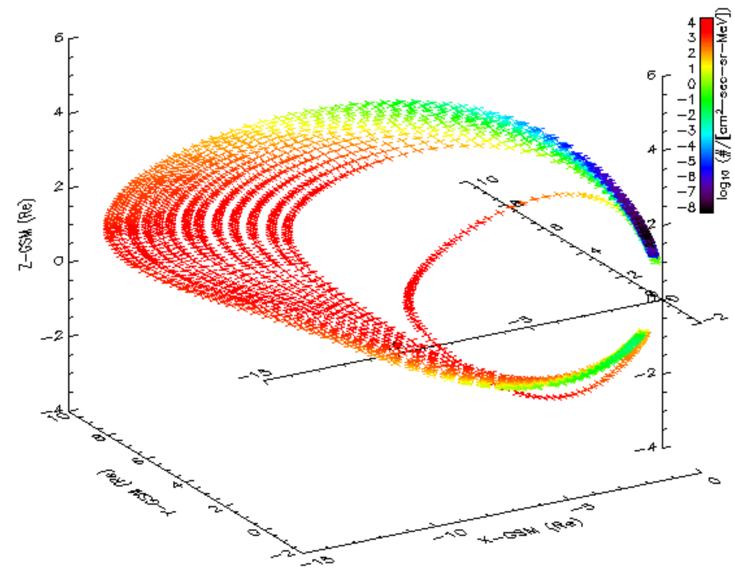

Day

- **X_{GSE} = 9 R_e, Y_{GSE} = 1 R_e, Z_{GSE} = 0 R_e**
- **Total flux points: 2191**
- **Restricted mapping points: ~393**

Night

- **X_{GSE} = -9 R_e, Y_{GSE} = -1 R_e, Z_{GSE} = 0 R_e**
- **Total flux points: 1978**
- **Restricted mapping points: ~579**

Streamline Mapping

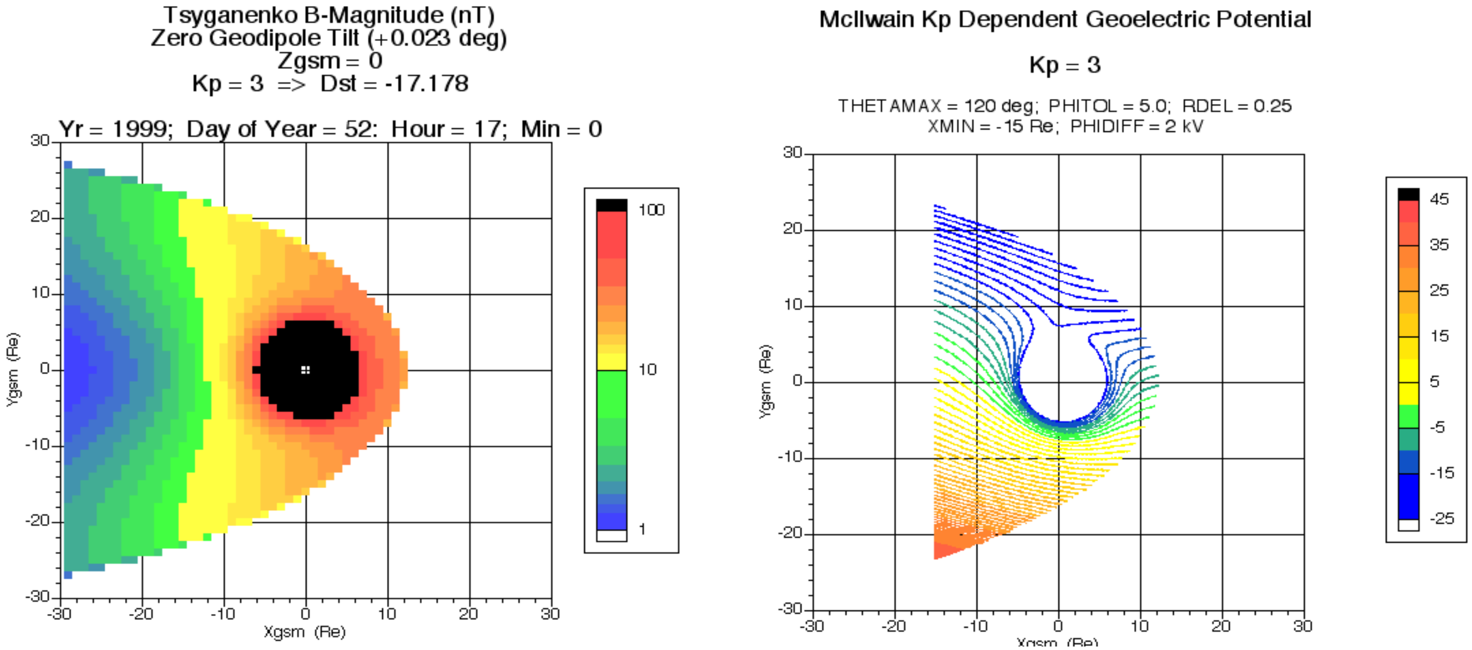

(a) **(b)**

Figure 4. Magnetic and Electric Potential Models. (a) Tsyganenko magnetic field intensity |B| (nT) and (b) geoelectric potential (kV) in the Z_{GSM} = 0 plane. These values will be used to compute an example set of streamlines shown in later figures.

- ExB drifts computed from magnetic field and Kp depdendent electric potential models

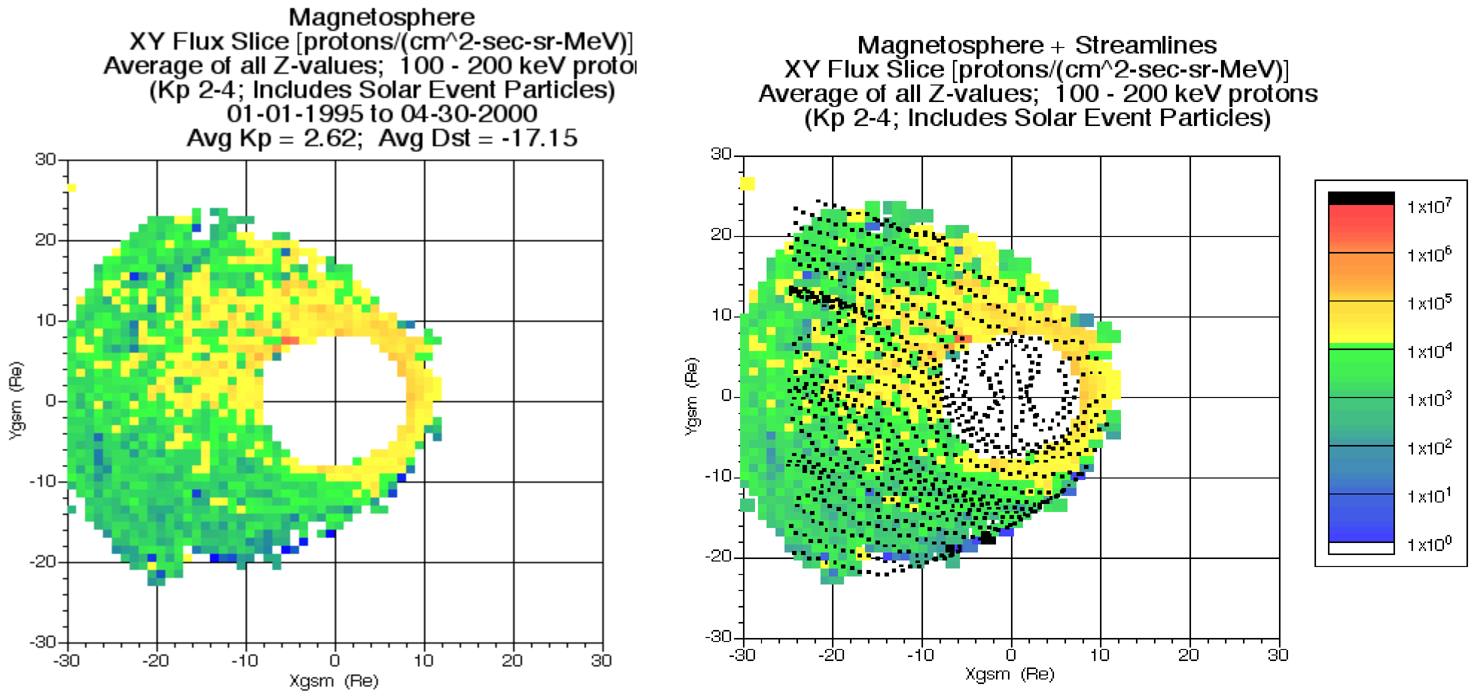

(a) **(b)**

Figure 6. Streamline Overlay on Magnetospheric Ion Flux Distributions. (a) Ion flux within the magnetosphere are projected onto the Zgsm = 0 plane. (b) Streamlines shown in Figure 2a are plotted over the ion flux distribution.

Example CRM Output

- Equatorial plane projection of CRM output for range of Kp values
- Model includes magnetosheath and solar wind

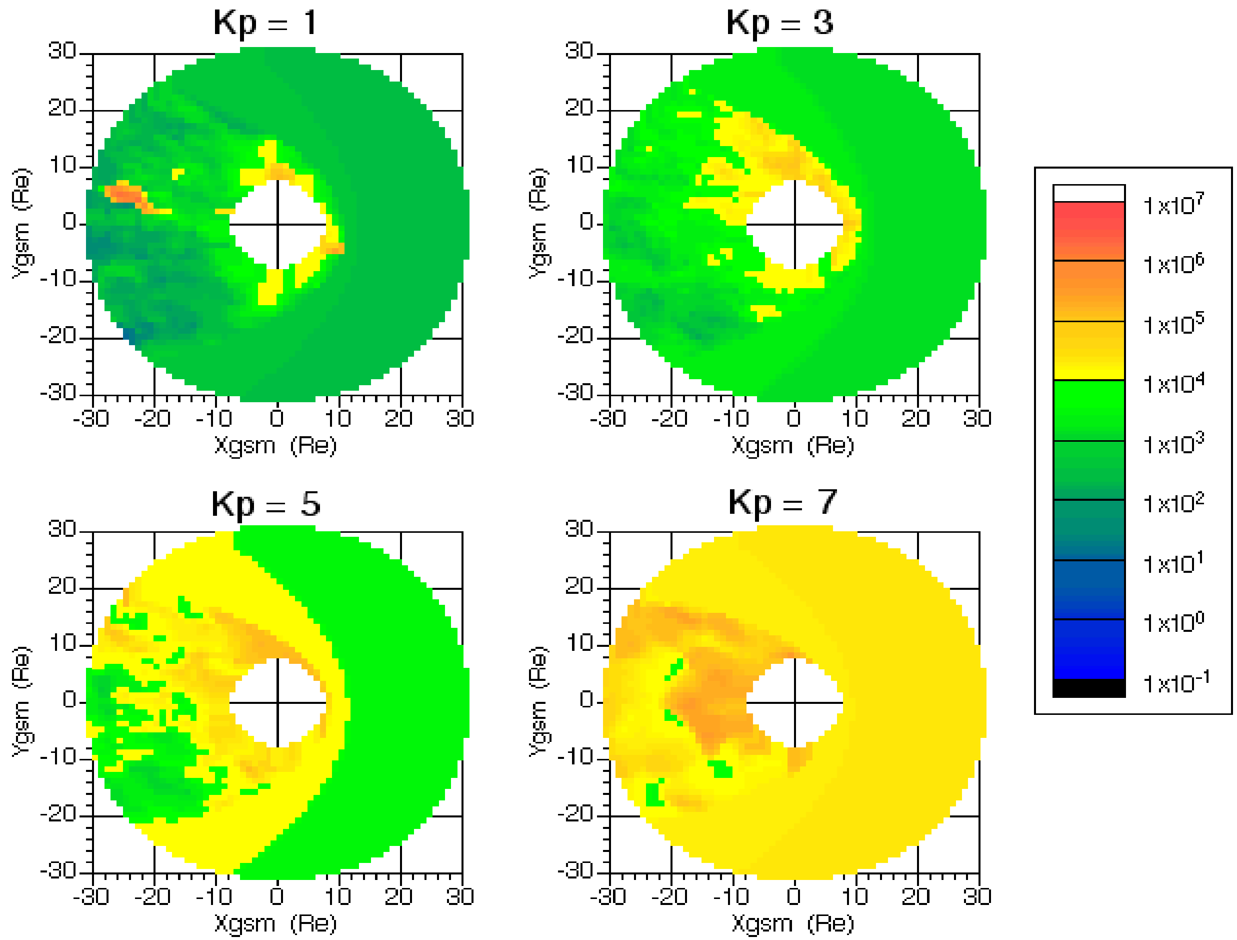

Figure 7. Ion Flux (protons/cm2-sec-sr-MeV) Output from CRM for a Range of K_p Values. Note the inward motion of the model magnetopause for higher Kp values (a property of the Tsyganenko magnetic field model) and the increase in flux.

CRM Modules

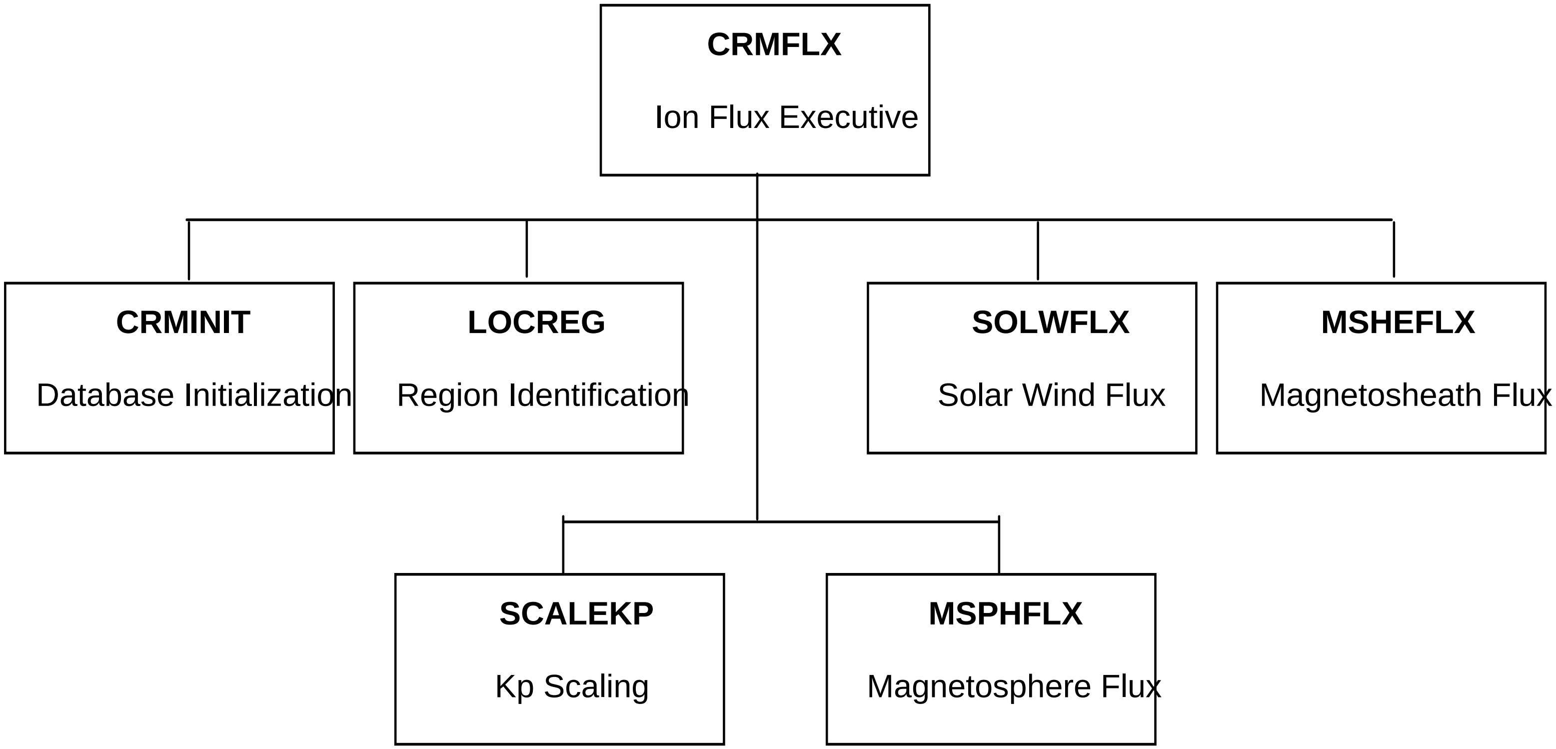

Figure 3. Major software modules in CRM.

Solar Proton Events

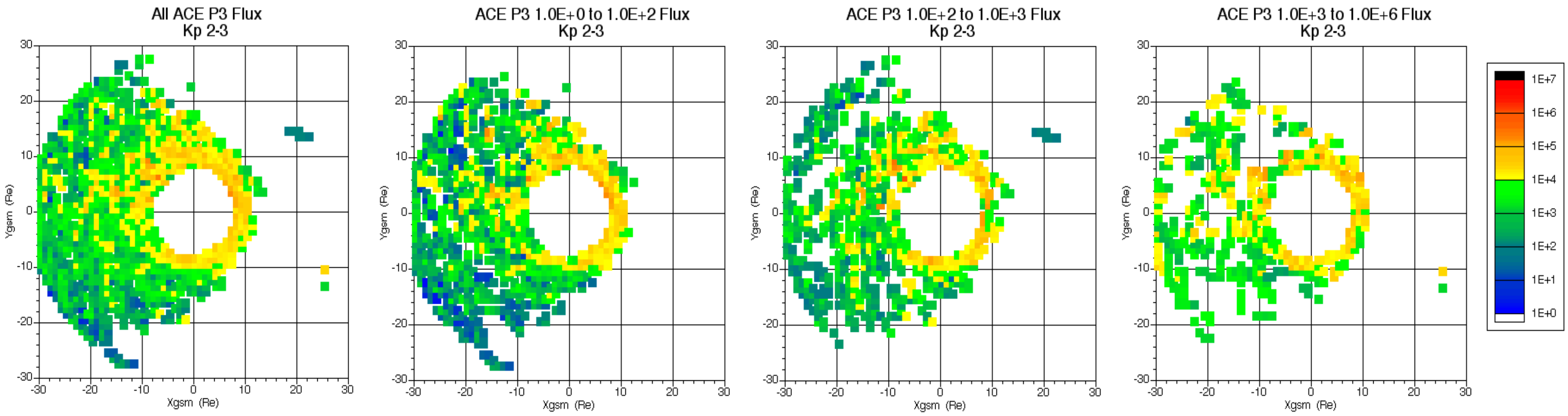

Figure 8. Solar Event Particle Correlation. *ACE* solar proton event correlation with *Geotail* flux data (units of protons/cm2-sec-sr-MeV) inside the magnetosphere for nominal Kp values. At low solar proton flux levels the data is dominated by the proton flux created by geomagnetic activity. At higher solar proton flux levels the solar event flux dominates in the outer magnetosphere.

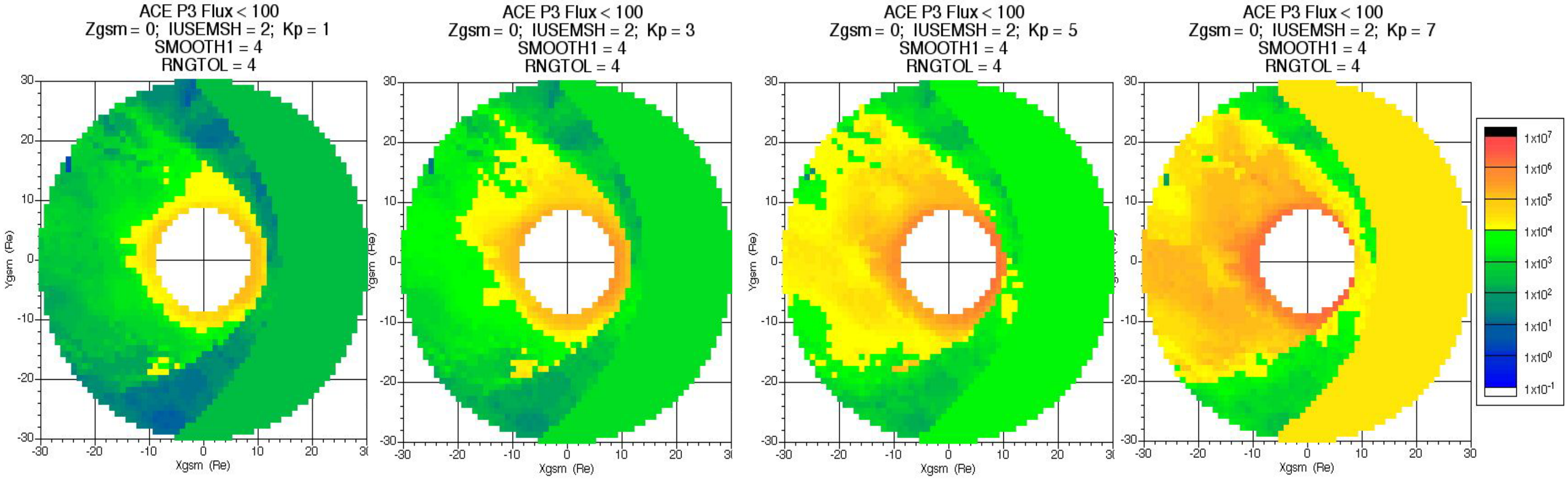
ACE P3 Flux < 100
Zgsm = 0; IUSEMSH = 2; Kp = 1
SMOOTH1 = 4
RNGTOL = 4
ACE P3 Flux < 100
Zgsm = 0; IUSEMSH = 2; Kp = 3
SMOOTH1 = 4
RNGTOL = 4
ACE P3 Flux < 100
Zgsm = 0; IUSEMSH = 2; Kp = 5
SMOOTH1 = 4
RNGTOL = 4
ACE P3 Flux < 100
Zgsm = 0; IUSEMSH = 2; Kp = 7
SMOOTH1 = 4
RNGTOL = 4
Ygsm (Re)
Xgsm (Re)
30
20
10
0
-10
-20
-30
$1x10^7$
$1x10^6$
$1x10^5$
$1x10^4$
$1x10^3$
$1x10^2$
$1x10^1$
$1x10^0$
$1x10^{-1}$

Fluence Scheduling

Average fluence (100-200 keV protons) per orbit for 2000

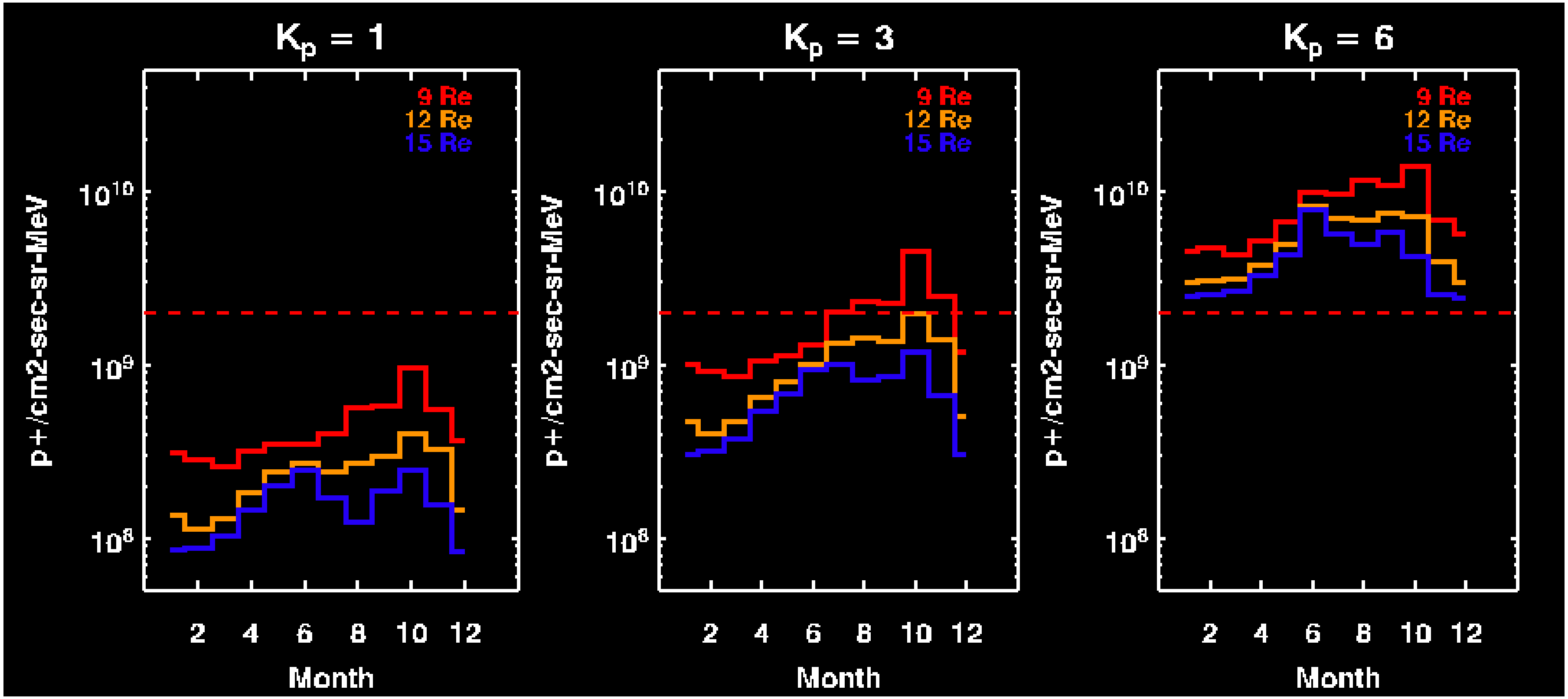

Fluence level to meet ACIS

5% CTI increase per year

Mission Fluence, CTi Estimate

- CRM Mission fluence

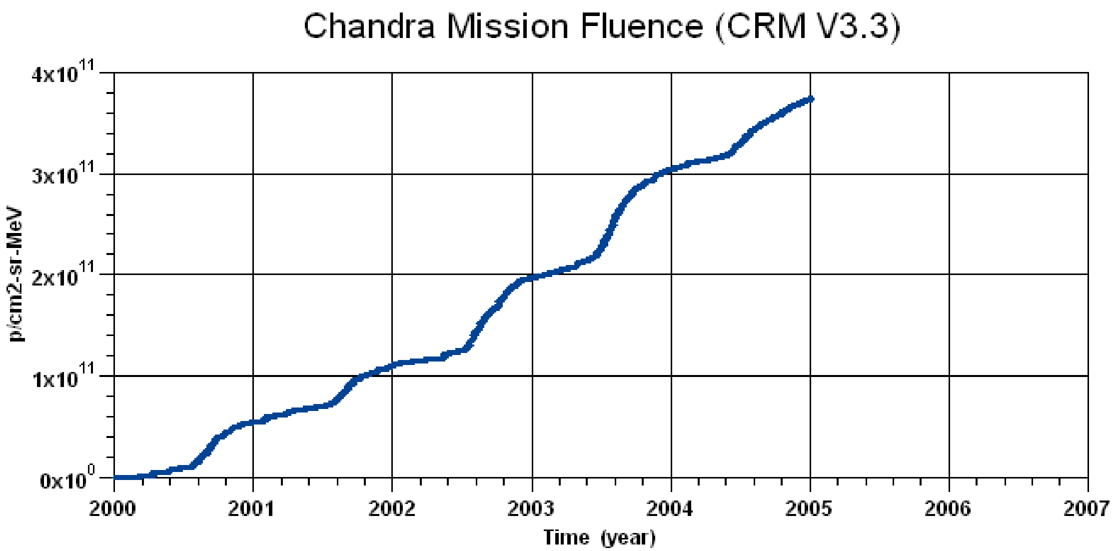

- Measured CTI and CRM predicted CTI
  - CTE increase ~ 2.3%/yr
    Requirement < 5%/yr

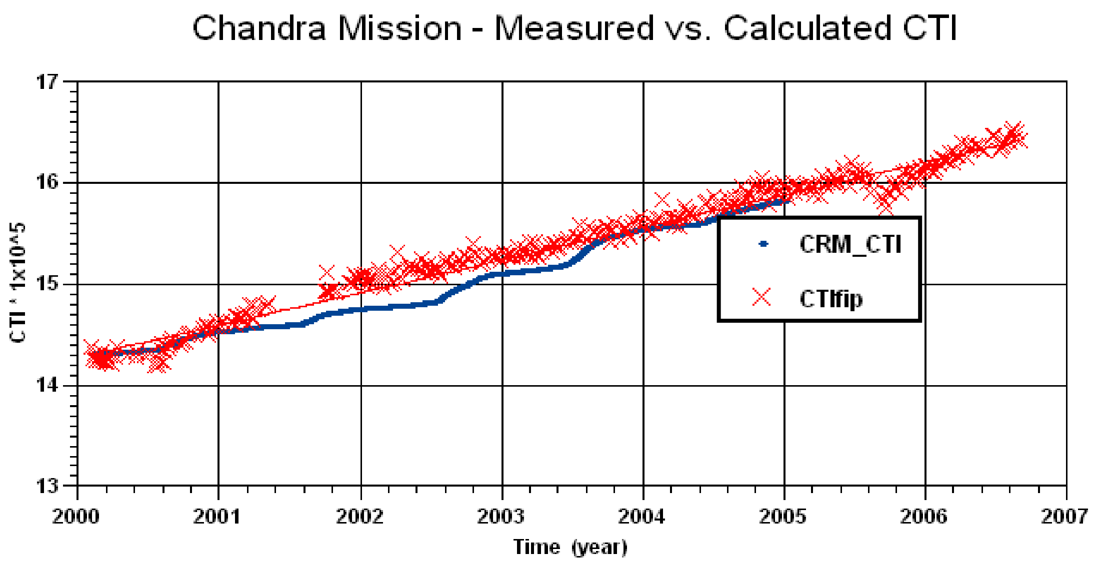

Summary

- CRM developed for Chandra program use in scheduling safe observation periods which avoid excessive radiation damage to ACIS detecto
- Model employs physics based mapping technique to fully exploit sparse data sets at high Kp
  - Geotail 1995 – 2004
  - Polar 1999 – 2004

Updates are planned to bring database up to date through 2008

- Current CTI increase running ~2.3%/year < 5% required to meet program objectives through end of mission